

Synthesis and Sintering Kinetics of Mechanically Alloyed FeCrCoMnNi High Entropy Alloy Powders

**A Dissertation Submitted to
Indian Institute of Technology Hyderabad
In Partial Fulfillment of the Requirements for
The Degree of Master of Technology**

By

Ashif Equbal

Roll No. MS13M1002

Under the supervision of

Dr. Bharat B. Panigrahi



**भारतीय प्रौद्योगिकी संस्थान हैदराबाद
Indian Institute of Technology Hyderabad**

**Department of Materials Science and Metallurgical Engineering
Indian Institute of Technology Hyderabad**

June, 2015

Declaration

I declare that this written submission represents my ideas in my own words, and where others' ideas or words have been included, I have adequately cited and referenced the original sources. I also declare that I have adhered to all principles of academic honesty and integrity and have not misrepresented or fabricated or falsified any idea/data/fact/source in my submission. I understand that any violation of the above will be a cause for disciplinary action by the Institute and can also evoke penal action from the sources that have thus not been properly cited, or from whom proper permission has not been taken when needed.

Ashif Equbal

ASHIF EQUBAL

MS13M1002

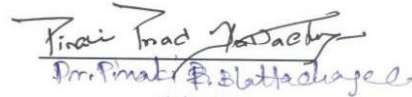
Approval Sheet

This thesis entitled "Synthesis and Sintering Kinetics of Mechanically Alloyed FeCrCoMnNi High Entropy Alloy Powders" by Ashif Eqbal is approved for the degree of Master of Technology from IIT Hyderabad.



Dr. Bhabani S. Malik
Dept of Chemistry
-Name and affiliation-

Examiner



Dr. Pinali Prad Kataria
MSME
-Name and affiliation-

Examiner



Dr. Bharat B. Panigrahi
MSME
-Name and affiliation-

Adviser



Dr. Saket Asthana
Dept. of Physics
-Name and affiliation-

Chairman

Acknowledgements

First of all, I am grateful to my thesis advisor Dr. Bharat Bhooshan Panigrahi for his constant guidance, support and motivation throughout the work, without which this would have not been materialized. I am grateful to all the faculty members of the department for their direct or indirect support during my thesis work and allowing me to use various instruments whenever required. I am thankful to Dr. P. P. Bhattacharjee for providing cast specimen for characterization and Prof. S. Kanagaraj of IIT Guwahati for extending their dilatometer facility. I am also thankful to my colleagues Raj Kumar and Rahul who worked with me all the time; and of course my all others seniors and colleagues who were always motivating and helping me in various ways; Akash, Zaid bhai, Krishna, Dan, Sushmita, Tushar, and all others.

Thank you very much.

Dedicated
to
My Brothers
Javed Akhtar
&
Ashique Equbal

Table of Contents

<u>Declaration</u>	
<u>Approval sheet</u>	
<u>Acknowledgement</u>	
LIST OF FIGURES	4
LIST OF TABLES	5
ABSTRACT.....	6
CHAPTER-1	8
INTRODUCTION	8
1.1 Introduction.....	8
CHAPTER 2.....	10
LITERATURE REVIEW.....	10
2.1 Fundamentals and Synthesis of HEA	10
2.2 Factors that affect behavior of High Entropy Alloys	14
2.3 Properties	15
2.4. OBJECTIVES OF THE PRESENT WORK	19
CHAPTER-3	20
EXPERIMENTAL PROCEDURE.....	20
3.1 Mechanical Alloying.....	20
3.2 Thermal treatment of mechanically alloyed powder	20
3.3 Dilatometer Sintering.....	21
3.4 Characterization.....	22
CHAPTER 4.....	23
RESULTS AND DISCUSSION	23
4.1 Synthesis of FeCrCoMnNi high entropy alloy through mechanical alloying.....	23
4.2 Heat treatment of milled powder	25
4.3 Sintering	30
CHAPTER 5.....	38
CONCLUSIONS	38
REFERENCES	39

List of Figures

FIGURE NO.	TITLE OF FIGURE	PAGE NO.
2-1	Schematic presentation of ternary and quaternary alloy phase diagram, showing regions that are relatively well known (black) near the corners and relatively less well known (white) near the center.	11
2-2	Vickers hardness and total crack lengths of the $Al_xCoCrCuFeNi$ alloy system with different aluminum contents (x values in molar ratio).	16
2-3	Compressive true stress-strain curves of $AlCoCrFeNiTi_x$ alloy	17
2-4	Thermal conductivities as a function of temperature (a), and as function of x in $Al_xCoCrFeNi$ alloys (b)	18
3-1	Schematic representation of shrinkage measurement from dilatometer plots	22
4-1	XRD patterns of 0h milled HEA mixed and elemental powder	23
4-2	XRD patterns of 0h 10h and 15h milled FeCrCoMnNi HEA powder	24
4-3	SEM micrograph of mechanically alloyed FeCrCoMnNi powders: (a) 10 h milled, and (b) 15 h milled.	24
4-4	DSC profile of 10h and 15h milled FeCrCoMnNi HEA heated at rate of 20°C/min	25
4-5	XRD patterns of 10h milled and heat treated at 400°C and 800°C.	27
4-6	XRD patterns of 15h milled and heat treated at 400°C and 800°C.	27
4-7	XRD patterns of 10h milled heat treated at 1100°C & elemental powder	28
4-8	XRD patterns of as cast HEA and 10h milled powder and heat treated at 1100°C	28
4-9	XRD patterns of as cast HEA and 15h milled powder and heat treated at 1100°C	29
4-10	SEM micrographs of sintered HEA powder at lower (a) and higher magnification (b); images of the indentation test at lower (c), and higher magnification (d)	30
4-11	Elemental mapping of selected area of sintered HEA sample	31
4-12	Dilatometer plot of the FeCrCoMnNi HEA sample sintered at 1150°C for isothermal holding of 1 h	33
4-13	Dilatometer plot of the FeCrCoMnNi HEA sample sintered at 1100°C for isothermal holding of 1 h	34
4-14	Dilatometer plot of the FeCrCoMnNi HEA sample sintered at 1000°C for isothermal holding of 1 h	34
4-15	Non-isothermal shrinkage obtained from dilatometer curves	35
4-16	Arrhenius plots to estimate activation energy for viscous flow	36
4-17	Arrhenius plots to estimate activation energy for volume diffusion	36
4-18	Arrhenius plots to estimate activation energy for GBD	37

LIST OF TABLES

TABLE NO	TITLE OF THE TABLE	PAGE NO.
4-1	Quantitative analysis of elements	32
4-2	Dimensional measurements of sintered sample at 1100°C	32
4-3	Activation energies obtained during non-isothermal sintering in the present work	37

ABSTRACT

High entropy alloys (HEAs) are solid solution of multi elements system fabricated in equi-atomic or near equi-atomic composition. These can be fabricated through two processing routes, melting-casting and mechanical alloying (MA). Objectives of this investigation are to synthesize the high purity single phase FeCrCoMnNi HEA powder through the mechanical alloying, and to study the sintering kinetics of this alloy powder.

Elemental powders of Fe, Cr, Co, Mn and Ni were taken in equi-molar ratio and milled up to 15 h using tungsten carbide vials and balls. XRD characterization of milled powders shows that high entropy alloy phase started forming at about 10 h of milling; mostly with FCC phase. Milled powders were further characterized using differential scanning calorimetry (DSC) to understand the phase formation behavior during heating. The DSC analysis indicates that the exothermic reactions were occurred at about 470°C, which may be attributed to the release of internal strains, accumulated during high energy ball milling and release of some dislocations and defects generated during milling. An endothermic peak at 990°C was observed, which could be attributed to melting of some intermetallics phases. Post-mechanical alloying annealing treatment up to 1000°C showed retention of the FCC phases.

Sintering experiments were carried out on 15 h milled powder, up to 1150 °C. Density of vacuum sintered sample was about 7.17 g/cm³ (relative sintered density of about 81%). To study the sintering kinetics, shrinkage as a function of time and temperature was recorded using vertical push rod dilatometer. The shrinkage data was analyzed through non-isothermal sintering models. The activation energies of various possible sintering mechanisms, such as viscous flow, volume diffusion and grain boundary diffusion were estimated during non-isothermal sintering and were found to be 13 kJ/mol, 37

kJ/mol and 56 kJ/mol respectively. The observed activation energies seem to very low for the complex alloy systems, indicating the contribution coming from high amount of dislocations and defects movements.

Keywords:

- High-Entropy Alloys,
- Mechanical Alloying,
- Powders,
- Sintering,
- Activation Energies.

CHAPTER-1

INTRODUCTION

1.1 Introduction

Alloys traditionally have been based on a solvent element to which various solute atoms are added for improving specific properties. An alloy may be a solid solution of the elements (a single phase), a mixture of metallic phases (two or more solutions) or an intermetallic compound with no distinct boundary between the phases. Unlike traditional alloys, recently a new type of alloy system has emerged where all the elements are principle elements present in equi atomic or near equi atomic composition. These alloy exhibit high configurational entropy therefore it is known as High Entropy Alloy (HEA). Usually it contains five or more metallic elements where each of these elements may have concentration in the range of 5 and 35 atomic percent [1]. It has high entropy of mixing ΔS_{mix} which is contributed by high configuration entropy ΔS_{conf} . It is well known in the alloy that even a small addition of new element in a system leads to change in the property drastically [2]. Even though the possibility to add more principal elements into the mixture has been always existed. When the alloy system moves from binary to ternary system, it contains several ordered phases, complex intermetallics and the derivatives of FCC, BCC, HCP phases etc. [2]. Complexity also increases and it becomes hard to control the phases. Surprisingly when multi-principal alloys were prepared, there were mostly disordered solid solutions with less number of compound formation than expected [1]. This was attributed to the aforementioned high entropy of mixing. It is known that the equilibrium phase of a system is decided by the lowest Gibbs free energy,

$$\Delta G_{\text{mix}} = \Delta H_{\text{mix}} - T\Delta S_{\text{mix}} \quad (1.1)$$

where H is the enthalpy, T is the temperature and S is the entropy. Another school of thought, Otto et al. [3] believes that only true solid solution forming multi-component alloys should be called high entropy alloys, since the multi-component alloys with intermetallic phases does not exhibit the full configurational entropy.

FeCrCoMnNi is among the initial high entropy alloy reported through the casting route. The properties of this HEA were to be superior to many other conventional alloys. Mechanical alloying route is one of the processing routes to synthesize such alloy which extends the solid solubility and control the microstructure. The aim of the present work is to synthesis of FeCrCoMnNi HEA powder via mechanical alloying (MA) and to study its behavior in different thermal condition. Also results were compared with the alloy produced through the casting route and found to be quite similar in context with the thermal behavior.

CHAPTER 2

LITERATURE REVIEW

2.1 Fundamentals and Synthesis of HEA

Ye et al [4] reported about the design of HEA and suggested a thermodynamic rule for the formation of HEAs, by maximization of the configurational entropy of mixing. They proposed a single-parameter design paradigm taking into account, formation enthalpy and the excessive entropy of mixing which arise from dense atomic packing and atomic size misfit. The proposed paradigm has been physically accepted thermodynamic parameter for the design of HEAs. In theory, the concept of “maximized configurational entropy of mixing out of equiatomic fraction” originates from an implicit assumption that atoms used to make up the alloy, have the identical size and are very loosely packed. This is similar to the case of an ideal gas whose configurational entropy of mixing merely depends on positioning of constituent elements. However, this is certainly not true for real alloys, in which the sizes of the constituent elements can differ by a large amount and the atomic packing is generally dense, which can form the cubic lattice or the hexagonal close packed lattice etc.

A schematic phase diagram of some hypothetical alloys have been shown in Fig 2.1. The information and understandings are highly developed on alloys close to the corners and edges of a multi-component phase diagram, whereas less information is available about the alloys located at the center of the phase diagram, as shown in the Fig 2.1. This imbalance is significant for ternary alloys but becomes rapidly much more pronounced as the number of components increases. For most quaternary and other higher-order systems, information about alloys even at the center of the phase

diagram is virtually nonexistent except those HEA systems that have been reported very recently. [2].

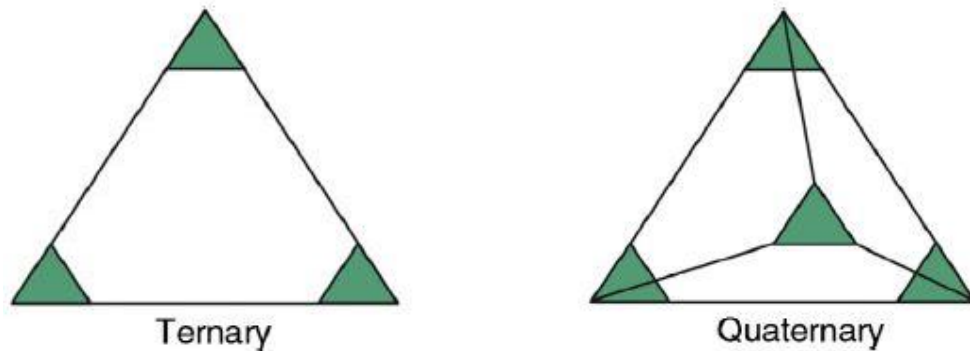


Figure 2-1: Schematic presentation of ternary and quaternary alloy phase diagram, showing regions that are relatively well known (black) near the corners and relatively less known (white) near the center. [2]

Brocq et al [5] first reported about phase diagram of very first HEA FeCrCoMnNi. In order to study the thermodynamics of high entropy alloys, the evolution of the structure and microstructure of the equimolar CrMnFe-CoNi high entropy alloy was investigated while processing under varying conditions (annealing duration and cooling rate). For the very first time, a true solid-solution down to the atomic scale was evidenced in an HEA by atom probe tomography.[5] It was shown that the FCC single phase solid solution was stable at high temperature in CrMnFeCoNi alloy. By analogy with completely miscible binary alloy, the CrMnFeCoNi HEA was described by a schematic phase diagram of the CrFeCo - MnNi system consisting of a liquidus and a solidus. It was reported that during fast cooling the microstructures of a single phase HEA were different than that of the slow cooled alloy. Also it was observed that while slow cooling alloy tends to have multiple phases rather than a single phase unlike fast cooling. When the liquid phase was cooled down, dendrites enriched in Co, Cr and Fe are formed and afterward interdendrites enriched in Mn and Ni solidified. The solid solution can be reached either by a very

fast cooling or by annealing the dendritic structure, for example at 1100°C for 1 h in CrCoFeMnNi HEA.

There are various processing routes adopted to synthesize these high entropy alloys. Though the arc melting route was widely reported synthesis route for HEAs, whereas the mechanical alloying is the only solid state route to synthesize HEAs. There are major advantages of MA route over arc melting route. Mechanical alloying method is known for its capability for extending the solid solubility limits and making the alloys of those metals which are difficult to form through conventional method. Also in mechanical alloying, it is possible to control on the grain size of the alloys by changing the milling parameters. Cantor [1] was reportedly the first to synthesize a very first high entropy alloy. He mixed twenty elements together in equal proportion and ended up with multi-phase alloy. However later on preparation of an alloy from five elements Fe, Cr, Co, Mn and Ni, was the breakthrough in alloying world and in 2004 this was a first single phase FCC high entropy alloy. Afterwards many research groups started working in this area and tried to synthesize with different processing routes. Mechanical alloying followed by spark plasma sintering, arc melting, cast and melt spinning are typical routes.

Yuhu et al. [6] reported the synthesis of AlNiCrFe_xMo_{0.2}CoCu high entropy alloy through powder metallurgy, i.e. mixing of elemental powders and sintering. Effects of Fe content on microstructure, hardness and comprehensive mechanical properties were investigated. Through the XRD analysis, it was shown that the constituent phases changed from BCC + FCC + σ at $x = 0.5$ to BCC + FCC at $x = 2.0$. The hardness of the alloys were found to be vary from HBW 3170 MPa at $x = 0.5$ to HBW 2290 MPa at $x = 2.0$. The fracture strengths of all the AlNiCrFe_xMo_{0.2}CoCu alloys were higher than 1100 MPa, and had exhibited a good plasticity. Wei Ji et al [7] developed FeCrCoMnNi high entropy alloy through mechanical alloying followed by spark plasma

sintering (SPS). As in SPS, cooling was done very fast; the HEA ended up with single phase FCC. During MA, a solid solution with refined microstructure of about 10 nm which consists of a FCC phase and a BCC phase was reported. After SPS consolidation, only one FCC phase was detected in the HEA bulks. Varalakshmi et al [8] reported in 2010, the synthesis and properties of nanocrystalline CuNiCoZnAlTi high entropy alloys by mechanical alloying. The CuNiCoZnAlTi high entropy alloy was mainly composed of BCC solid solution with crystallite size less than 10 nm in as milled condition. This alloy powder was consolidated using vacuum hot press at 800 °C with 30 MPa pressure to a density of about 99.9%. This alloy was thermally stable at elevated temperature about 800 °C as it was found to retain its nanostructure. The hardness and compressive strength of the high entropy alloy were found to be 7.55 GPa and 2.36 GPa, respectively. Superior strength of high entropy alloy was attributed to the solid solution strengthening and its nanocrystalline nature. Because of the unique property of these HEAs, various combination are being constantly tried to get a new alloy. Early transition elements, late transition elements, refractory elements were different combination reported by different research groups. Chen et al [9] reported about $\text{Al}_{0.5}\text{CrFeNiCo}_{0.3}\text{C}_{0.2}$ high entropy alloy processed by mechanical alloying and spark plasma sintering. Along with the metallic system, carbon was introduced. During the MA process, a supersaturated solid solution with both face-center cubic (FCC) and body-center cubic (BCC) structures was formed within 38 h of milling. However, a major FCC phase, a BCC phase, Cr_{23}C_6 carbide and an ordered BCC phase were also observed after SPS. The FCC phase was enriched with Fe–Ni, the BCC phase was enriched with Ni–Al and the ordered BCC phase was especially enriched with Al, respectively. In addition, nanoscale deformation twins were also found in partial FCC phase after SPS. The compressive strength and Vickers hardness of $\text{Al}_{0.5}\text{CrFeNiCo}_{0.3}\text{C}_{0.2}$ high entropy alloy were reported to be of 2131 MPa and 617 ± 25 HV, respectively.

2.2 Factors that affect behavior of High Entropy Alloys

There are four major factors seem to affect the HEA behavior. [10]

i) **High mixing entropy effect**

The higher amount of elements in a disordered state may give rise to an entropy that may suppress many intermetallic phases and other ordered phases, especially at elevated temperatures since the entropy contribution to the Gibbs energy in equation (1.1) scales with temperature, while the enthalpy does not.

ii) **The sluggish diffusion effect**

It was reported that diffusion in HEAs works slower than the conventional alloys. If one imagines a lattice built up of several different elements, then the atom diffusing from one spot to a neighboring spot, will most likely be in an environment quite unlike its previous spot, with different elements in the neighboring spots and therefore a different potential energy. It might be possible that if the potential energy of new spot is higher, than the atom may return to its original spot. If the new spot is energetically preferable, the atom continues its journey to another step. But there will also be spots where, it will take more energy to pass, i.e. the potential energy will fluctuate from spot to spot due to the different neighboring elements. This sluggish diffusion indicates that many HEAs may have excellent high-temperature properties, with good creep resistance and strength properties.

iii) **Lattice distortion effect**

A lattice consisting of atoms of different radii will become distorted, with larger atoms pushing on neighboring sites and smaller atoms will have more free space in their vicinities. This distortion may hinder dislocation movement and thus lead to the solid solution strengthening. It will also affects the

scattering of propagating electrons and phonons, meaning that the electrical and thermal conductivities will be affected.

iv) **Cocktail Effect**

Basically it says that the properties of HEAs cannot just be taken from averaging the properties of the constituting elements. There will also be some effects on the properties from the interaction between different elements and phases as well as from the lattice distortion effect, this cocktail effect then gives many possibilities for materials with different properties.

2.3 Properties

2.3.1 Strength

AlCoCrCuFeNi system is among the widely studied HEAs. Early studies showed the effect on strength by varying content of aluminium concentration for the arc-melted and cast system [11], and changing the aluminium content changed the crystal structure of the alloy [12] and also changes the strength. Normally a FCC phase is considered softer and more resistant to change under elevated temperatures, while a BCC phase is harder and more sensitive to high temperatures. For lower Al content there is a rather ductile FCC phase while increasing it will introduce an ordered bcc phase. More Al addition increased the strength of the alloy while lowered its ductility. The hardness ranges from ≈ 100 to 600 HV (see Fig. 2.2). The strengthening was attributed to the solid solution strengthening with the larger Al-atoms, precipitation strengthening of nanophases as well as increasing the ratio of the stronger BCC phase [13].

The effect of titanium addition on AlCoCrCuFeNi and AlCoCrFeNi system were also investigated. [11]. At lower concentration of Ti in AlCoCrFeNi (alloy without copper) there were two BCC phases whereas at higher concentrations of titanium a Laves phase formed. It showed a high strength (Figure 2.3 shows the true stress strain curves for AlCoCrFeNiTi_x for some values of x) particularly, the AlCoCrFeNiTi_{0.5} alloy had a compressive yield strength of 2.26 GPa, a fracture strength of 3.14 GPa and a plastic strain of about 23.3% [14]. This system gets its strength from BCC solid solution strengthening, precipitation strengthening and nano-composite effects etc. [15]. When the concentration of Co was raised one of the BCC phase transformed to a FCC phase which lowered the strength [16].

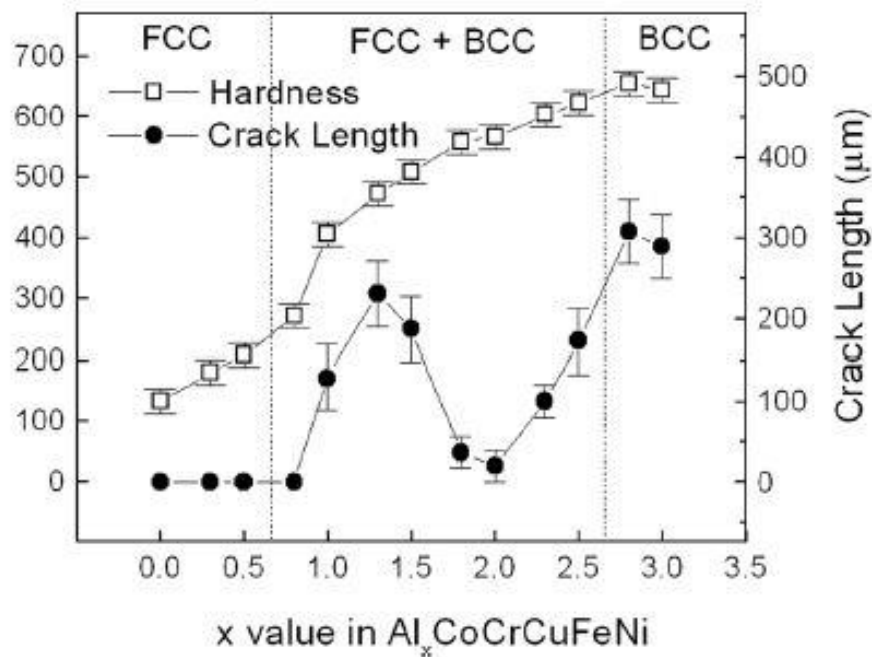


Figure 2-2: Vickers hardness and total crack lengths of the Al_xCoCrCuFeNi alloy system with different aluminum contents (x values in molar ratio). [11].

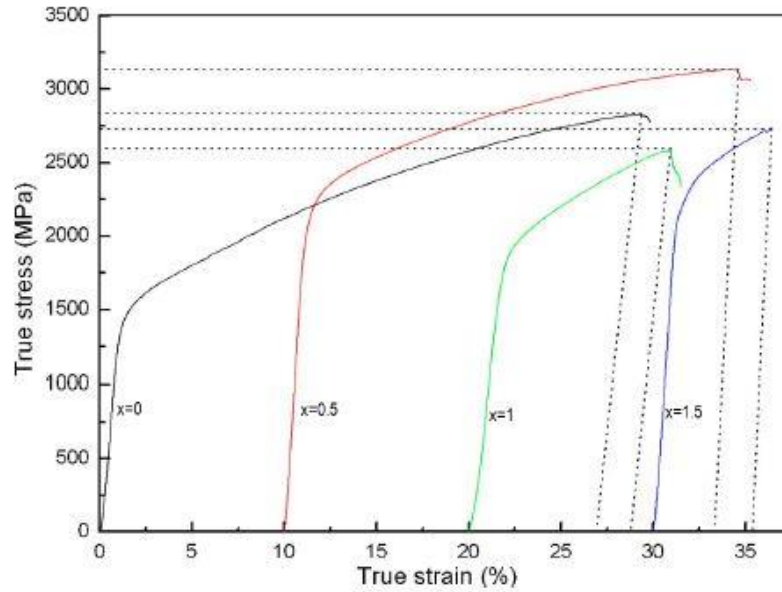


Figure 2-3: Compressive true stress-strain curves of AlCoCrFeNiTi_x alloy [14]

2.3.2 Thermal properties

Thermal conductivity of $\text{Al}_x\text{CoCrFeNi}$ has been shown in Figure 2.4(a), where it was found that the thermal conductivity was similar to that of the superalloys. Unlike pure metals where thermal conductivity decreases with increased temperature; it increases in HEAs. This was attributed to the increase in lattice size from thermal expansion, giving the electrons a larger mean free path before scattering, as well as due to a smaller carrier concentration. [17].

2.3.3 Magnetic and Electric Properties

Magnetic properties of HEAs have been studied by several researchers. It was seen that AlCoCr-CuFeNi showed good soft magnetic behavior with high saturated magnetization (M_s) and low coercivity (H_c) [18], both of which increased after aging [19]. The ferromagnetic behavior of AlCoCrCuFeNi was correlated with the spinodal decomposition of the Cr-Fe-Co rich regions into

ferromagnetic Fe-Co-rich and anti-ferromagnetic Cr-rich domains [19]. It was also found that addition of tungsten made it partially paramagnetic, while adding zirconia made it completely paramagnetic [20]. The electrical resistivity is much higher than that of the relevant pure metals, which was attributed to the lattice distortion effect [21]. It was also noted that after annealing the resistivity increased even more due to the appearance of more intermetallic phases [11].

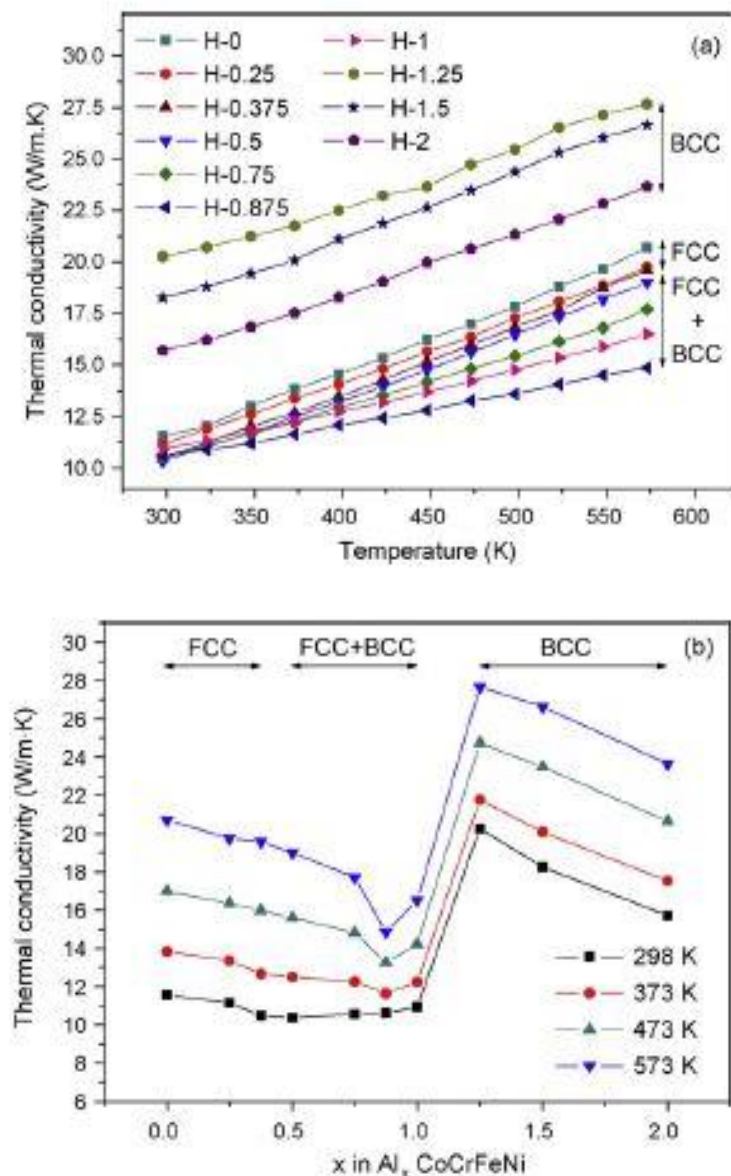


Figure 2-4: Thermal conductivities as a function of temperature (a), and as function of x in $Al_xCoCrFeNi$ alloys (b) [11].

2.3.4 Thermo-mechanical processing

Bhattacharjee et al [22] reported about the thermo-mechanical processing and property of FeCrCoMnNi HEA. They studied about microstructure evolution and texture after heavy cold rolling and annealing at various temperature ranges. After 90% of cold rolling a strong brass type texture was observed. An ultrafine microstructure having average recrystallized grain size of 1 μm with profuse annealing twins was observed after annealing at 650°C. Remarkable resistance against grain coarsening was observed at least up to 800°C. The mechanisms for these features were closely related with the distinct whole-solute matrix in HEAs. The recrystallization texture was characterized by the retention of deformation texture components similar to those of TWIP and 316 stainless steels. But notable differences exist. It could be attributed to profuse annealing twin formation due to the low stacking fault energy of the alloy.

2.4. OBJECTIVES OF THE PRESENT WORK

The critical review of the literature indicates that varieties of study on synthesis and properties of HEA have been reported. Powder were produced through mechanical alloying route and sintered. However it is evident that many of issues have not yet fully understood, such as diffusion behavior and sintering mechanisms, etc. Therefore following objectives have been chosen for current study:

- i) To synthesize the single phase FeCrCoMnNi high entropy alloy through mechanical alloying.**
- ii) To study the phase stability and phase evolution during annealing.**
- iii) To study the sintering kinetics of milled HEA powder.**

CHAPTER-3

EXPERIMENTAL PROCEDURE

3.1 Mechanical Alloying

Mechanical alloying is solid state synthesis route to produce nano crystalline powder. The mechanism behind MA is to reduce the particle size by ball milling because of collision of powders with the tungsten ball. Reduction in particle size leads to increase in the surface area followed by decrease in activation energy of the powder. That leads to increase in reactivity of the powder. Elemental powders of Fe, Cr, Co, Mn with mesh of sizes -325 and about 99% purity were procured from Alfa Assar and the nickel powder with mesh size of -325 and about 99.5% purity was procured from Sigma-Aldrich. About 40 g of powders were taken in equi-molar ratio of 20 % each and powder were converted into weight percentage of 19.91%, 18.54%, 21.015%, 19.59%, 20.93% respectively. Then these powders were kept in high energy planetary ball mill system (Fritsch P-5) for mechanical alloying. The vials and ball were made of tungsten carbide. Balls used were of different sizes had diameter of 15 mm and 10 mm. Toluene was used as a process control agent to avoid oxidation of powder and to minimize the heat generation. Ball to powder weight ratio was taken as 10:1 and milled at a speed of 300 rpm. Powders were taken after 10 h and 15 h for characterization and further study. 15 h milled powder was selected for sintering study.

3.2 Thermal treatment of mechanically alloyed powder

To understand the phase stability and phase evolution behavior of mechanically alloyed powder, Differential Scanning Calorimetry analysis has been performed. Differential Scanning calorimetry (DSC:

NETZSCH DSC 404F3) was done up to 1450°C while heating at a rate of 20 K/min. For thermal treatment pellets were made from the powders by compacting at a pressure of around 50 MPa using 10 mm diameter cylindrical steel die and punch. Subsequently these powder were heated at 400°C, 800°C and 1100°C with a heating rate of 15°C/min in inert atmosphere (Argon) and were hold for 1 h.

Two different sets of sintering operations were carried out: (i) in vacuum furnace and (ii) in dilatometer. For sintering, cylindrical compacts of 10 mm diameter were prepared by compacting at a pressure of 50 MPa. Sintering was performed at 1100°C with a heating rate of 15°C/min for 1 h in vacuum (4.1×10^{-5} mm of Hg).

3.3 Dilatometer Sintering

For the dilatometer experiments compacts of 7 mm diameter were prepared by compacting at 50 MPa. The compact had a green density of 4.7g/cm³. Sintering of samples were carried out in a Single push rod (vertical) Dilatometer (Dilamatic II, Theta Industries US). After inserting sample, first of all dilatometer tube were evacuated for 10 minutes followed by purging of Ar for 30 minutes to ensure the inert atmosphere during sintering. For all the samples, same heating rate of 10°C/min was employed. Samples were heated to 900°C to 1150°C for an isothermal holding of 1 h, followed by the furnace cooling. The major purpose of dilatometer study was to observe the shrinkage behavior as a function of temperature and time.

Push rod dilatometer serves the measurement of the change in length as a function of temperature. Dilatometry is the method for precise measurement of dimensional change of solid compacts at a programmed temperatures and over a range of time with negligible sample strain (ASTM E831, ASTM D 696). Hence dilatometry has been used for the long time to monitor the sintering behavior of powder

compacts. Dilatometer sintering plot can be evaluated in two different region, i.e. non-isothermal part and isothermal part. During non-isothermal sintering, temperature is continuously increased at a constant heating rate, while in isothermal sintering temperature is kept constant for the range of time. A schematic presentation of shrinkage measurement method has been shown in figure 3.1.

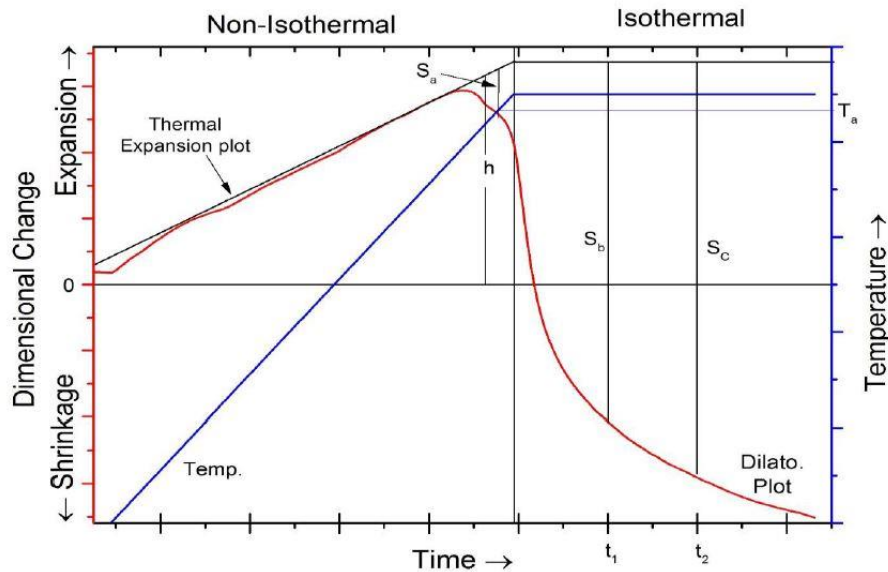


Figure 3-1: Schematic representation of shrinkage measurement from dilatometer plots

3.4 Characterization

Materials were characterized at every stage of processing. XRD of all the milled samples (10 h and 15 h) were carried out on X-ray diffractometer (PANalytical, Model: X'Pert PRO) with Cu k_{α} radiation of wavelength 1.54 \AA as a source, step size of 0.002 degree of 2θ at slow scan rate (total scanning period of about 1h). To observe surface morphology of HEA SEM images of all the milled powders were taken at different resolution using FEG-SEM (Carl-Zeiss, Model: Supra 40). SEM micrographs of sintered samples have been taken to study the microstructure. Also EDAX were carried out to study the atomic percentage of all the elements in the HEA powder and also elemental mapping were carried out to study the distribution of the elements.

CHAPTER 4

RESULTS AND DISCUSSION

4.1 Synthesis of FeCrCoMnNi high entropy alloy through mechanical alloying

Figure 4.1 shows the XRD patterns of the milled powders collected for elemental powders and 0 h milled powder (i.e. mixed powder before milling). Patterns show individual peak positions of each elements at their respective positions.

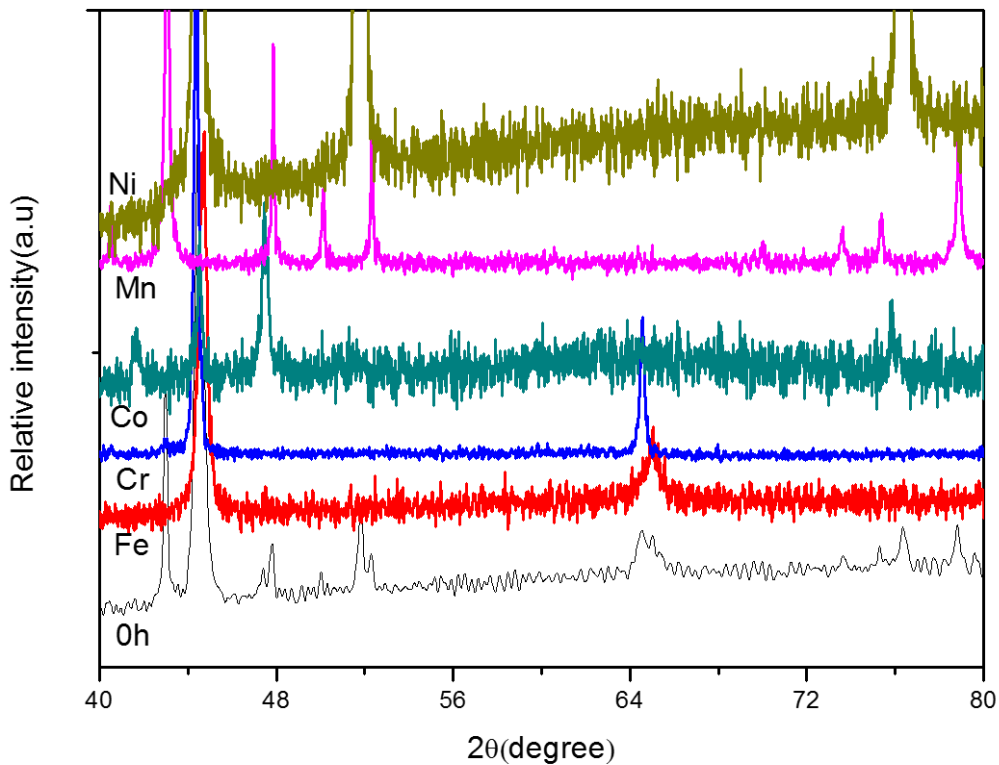


Figure 4-1: XRD patterns of 0 h milled HEA (mixed powder) and elemental powders.

Figure 4.2 shows XRD patterns of milled powders. Alloy seems to be forming in 10 h of milling. Peaks corresponds to individual elements were vanished indicating the formation of alloys. Since in many literature it has been reported that during MA it forms FCC or BCC

phases. Four strongest peaks were found to be identical to the patterns of FCC crystal system, such as pure nickel. However peaks were relatively broader than the usual pure metal. The trend observed for 10 h during XRD analysis, remained the same for 15 h milled powder also, as shown in Fig 4.2.

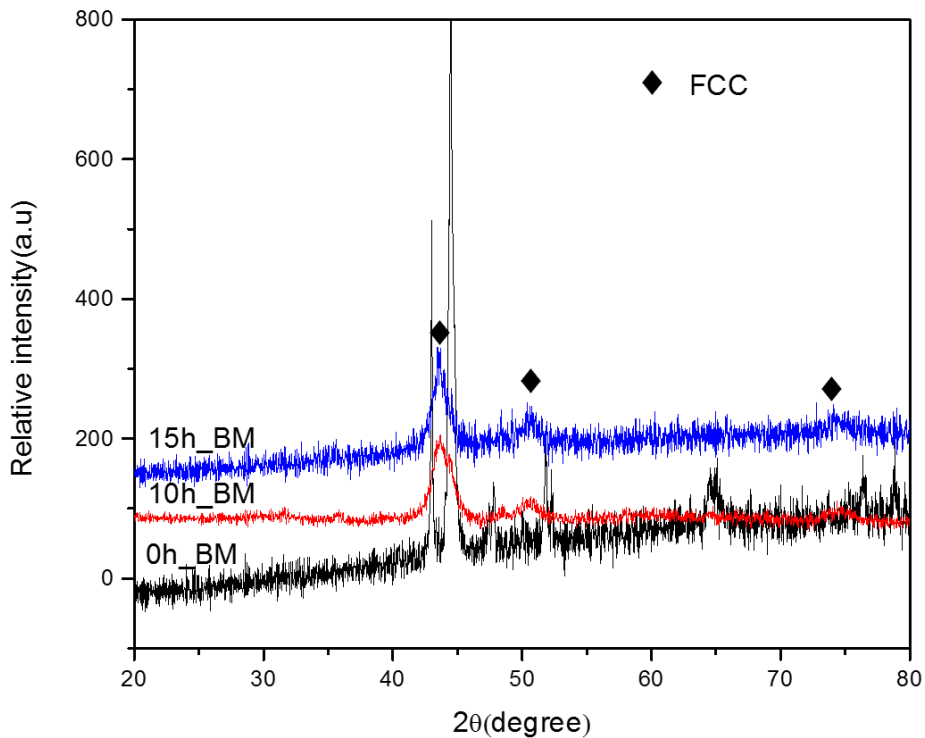


Figure 4-2: XRD patterns of 0h 10h and 15h milled FeCrCoMnNi HEA powders.

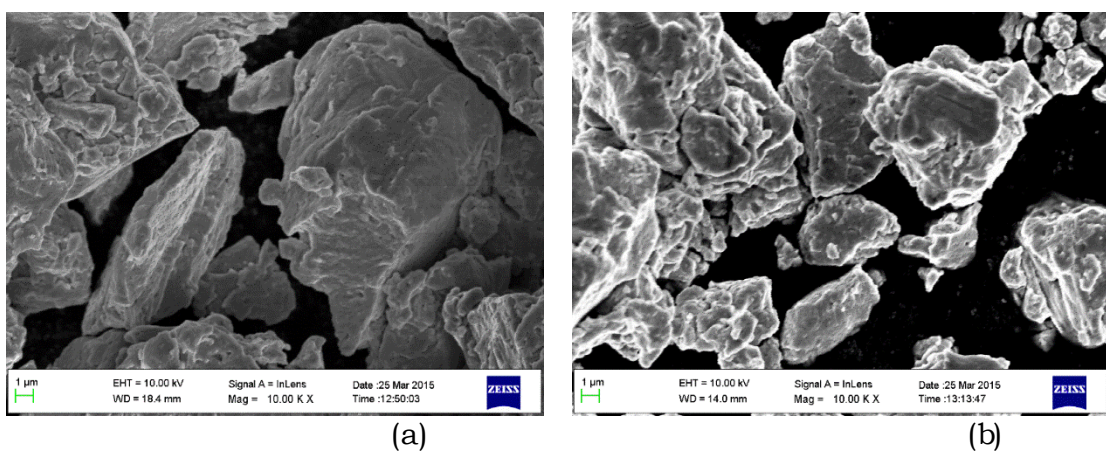


Figure 4-3: SEM micrographs of mechanically alloyed FeCrCoMnNi powders: (a) 10 h milled, and (b) 15 h milled.

Figure 4.3 shows SEM images of 10 h and 15 h milled FeCrCoMnNi powders; showing the particle size reduction with increasing milling hours. Shapes of powders were non-uniform throughout and layering of crystallites were observed. Sizes of particles were very fine but highly agglomerated.

4.2 Heat treatment of milled powder

The phase stability of mechanically alloyed powder of 10 h and 15 h was characterized through DSC analysis, which have been shown in Fig 4.4.

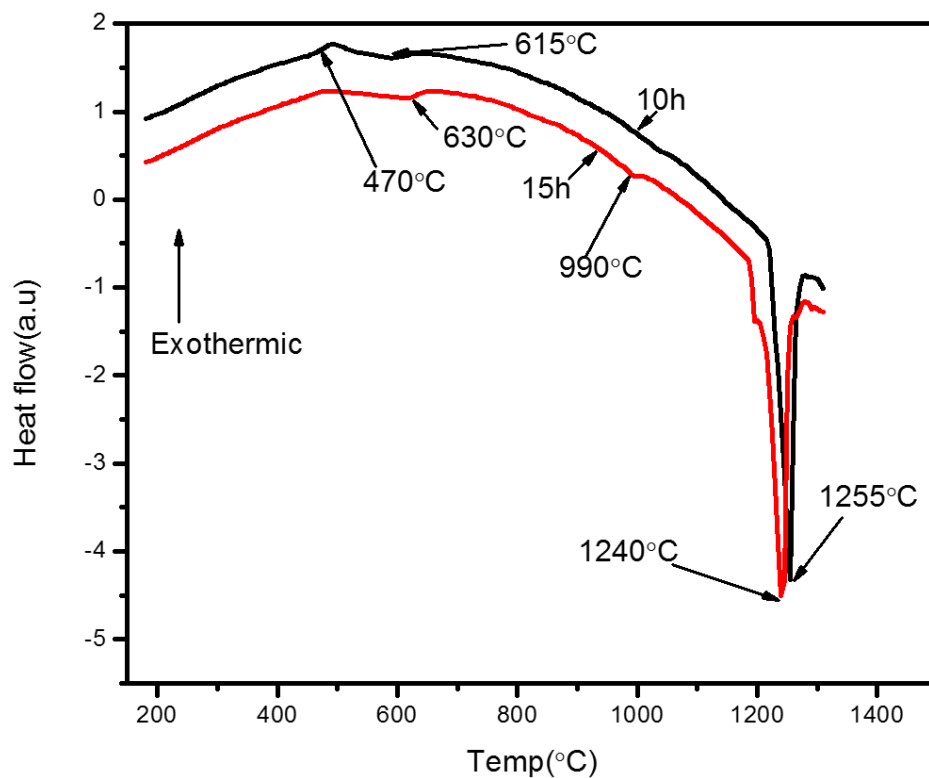


Figure 4-4: DSC profiles of 10h and 15h milled FeCrCoMnNi HEA heated at a rate of 20°C/min.

Four different peaks were observed during heating. Since powder was milled under high energy ball mill, materials must have accumulated with high amount of dislocation, defects and strains. Thus the exothermic peak at 470°C may be attributed to the release of internal strains and dislocations of milled powder. The exothermic behavior of curve after 470 °C, may be related to the secondary reactions and phase homogenization in the partially reacted and mechanically alloyed phases. At about 990°C, an endothermic peak was detected, an indication of melting of some phase. It is possible that during milling of five elements, some minute amount of other phase or intermetallic might have formed. At high temperature of about 1255 °C in 10 h milled and 1240 °C in 15 h milled, an endothermic peak was observed, attributed to the melting of the alloy.

After DSC analysis of milled powder, heat treatment were done at 400 °C, 800 °C and 1100 °C and characterized the phases through XRD. During the heat treatment major phase remained FCC and seems to be stable at elevated temperatures as shown in Fig. 4.5 and 4.6. All the above XRD profiles and DSC profiles were further compared with that of the as-cast high entropy alloy; interestingly the phase observed during mechanical alloying was similar to that of as-cast alloy. Figure 4.7 shows the XRD pattern of 10h milled and heat treated at 1100°C powder and all the elemental powders together to compare the phases. It has been clearly shown that 10 h milled and heat treated sample was single FCC phase where patterns were identical to the peaks of Nickel.

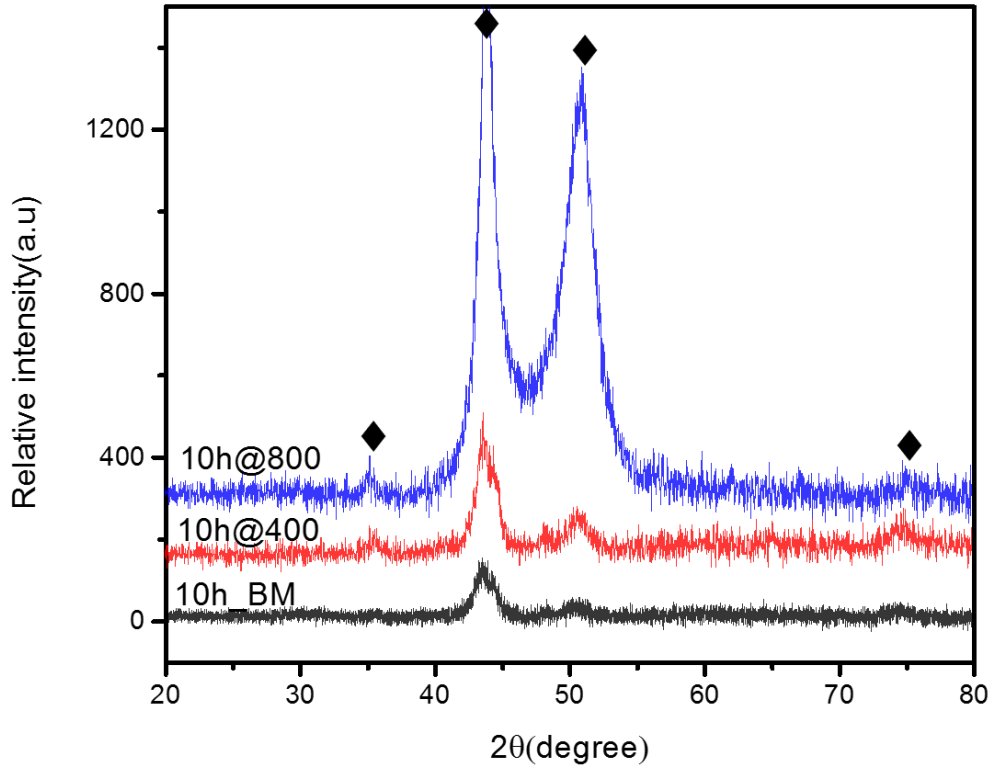


Figure 4--5: XRD patterns of 10h milled and heat treated at 400°C and 800°C.

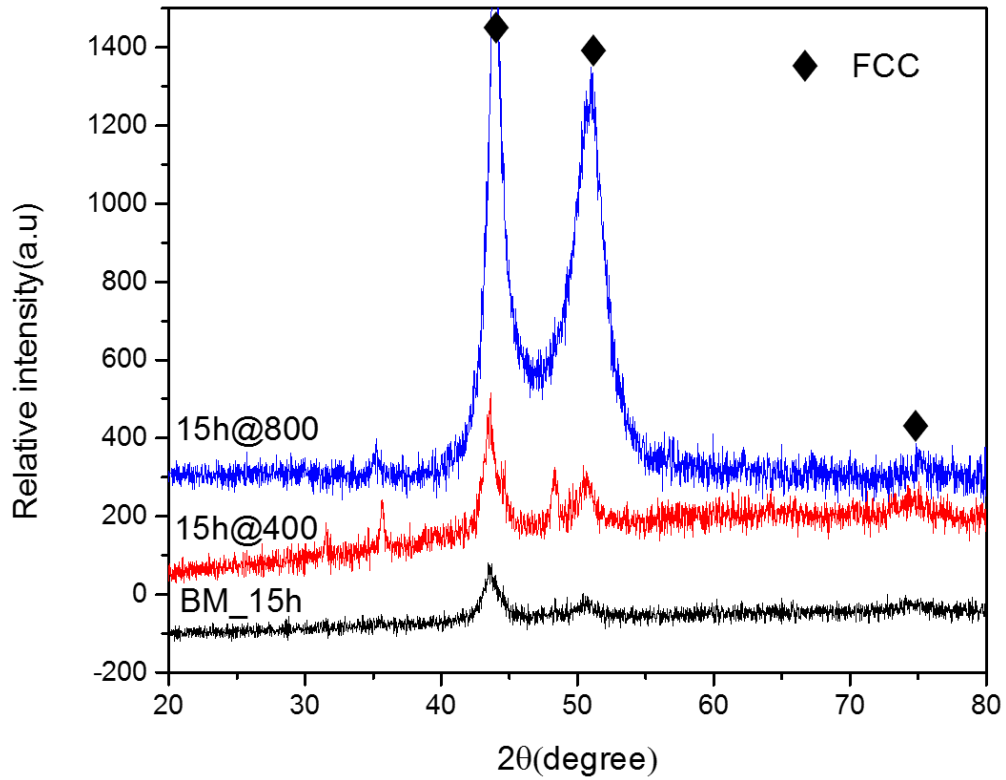


Figure 4-6: XRD patterns of 15h milled and heat treated at 400°C and 800°C.

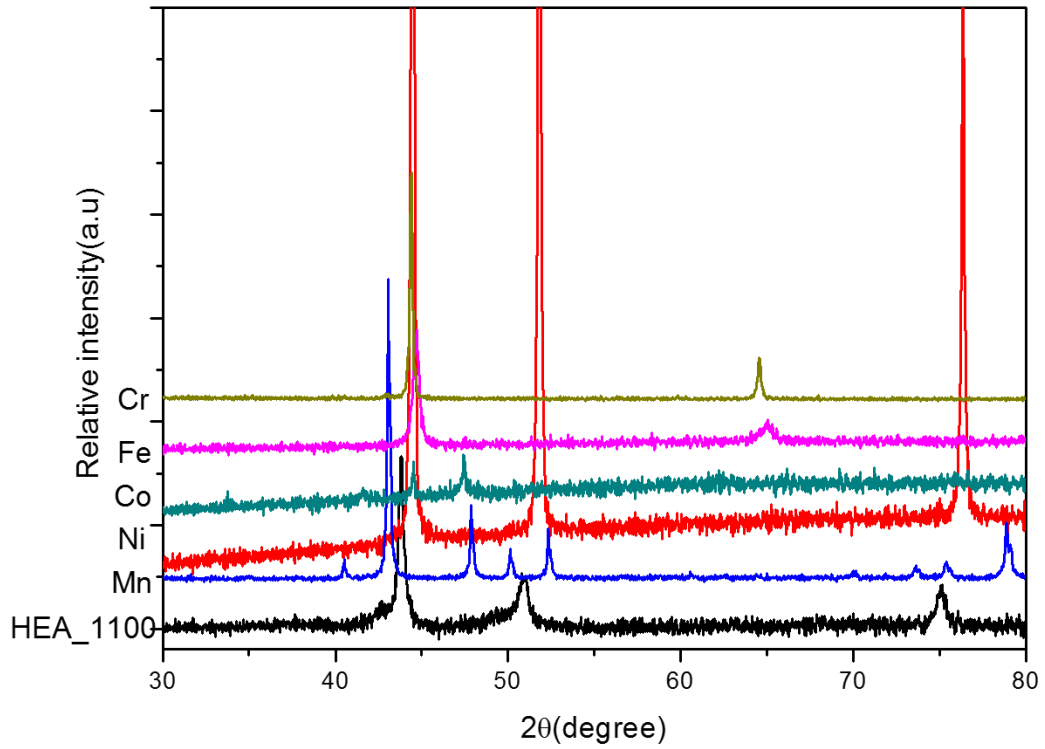


Figure 4-7: XRD patterns of 10h milled heat treated at 1100°C & elemental powders.

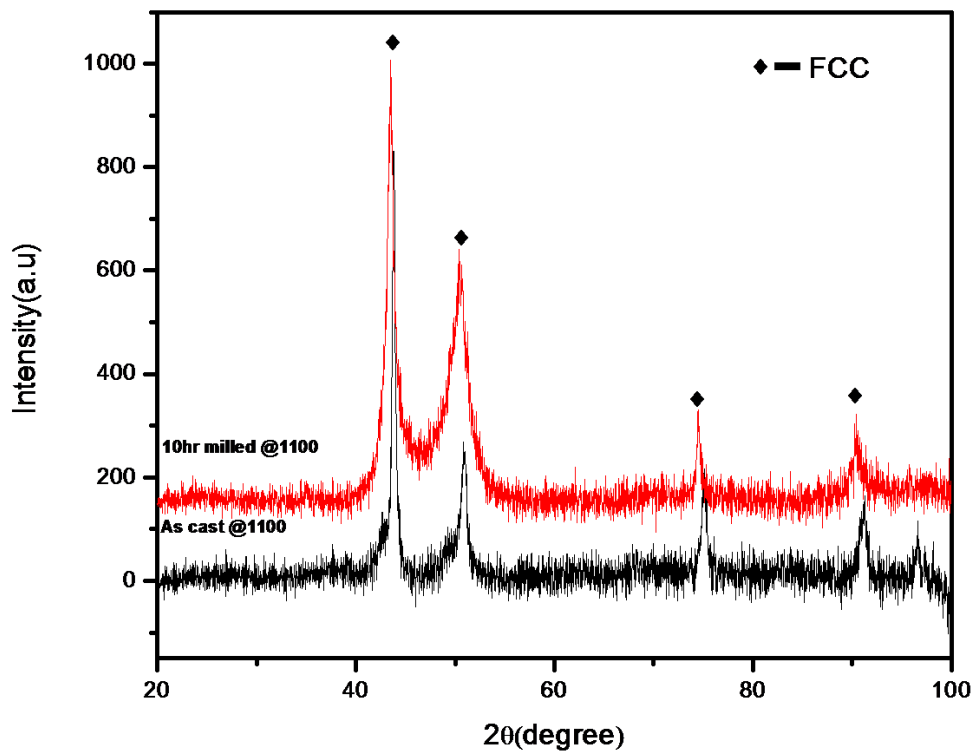


Figure 4-8: XRD patterns of as cast HEA and 10h milled HEA powder heat treated at 1100°C.

In Fig 4.8 it has been shown that XRD profiles of 10h milled and heat treated at 1100°C HEA are exactly matching with the cast-HEA under similar heating conditions. Which confirms that 10h milled HEA is single phase FCC. Same behavior has been observed by 15h of milled HEA powder. XRD plot of 15h heat treated HEA at 1100°C and as cast HEA has been shown in Fig 4.9. Result shows a very similar behavior of 10h milled and 15h milled HEA powders.

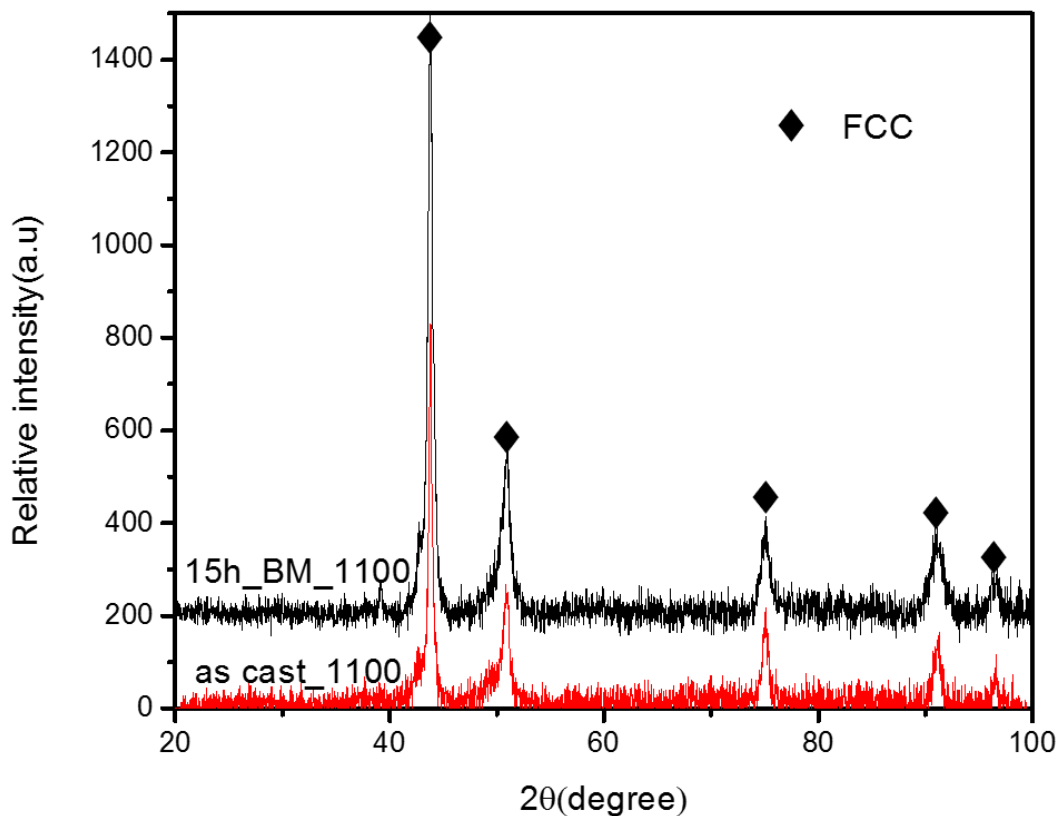


Figure 4-9:XRD patterns of as cast HEA and 15h milled powder and heat treated at 1100°C

4.3 Sintering

After synthesis of HEA powder two different sets of sintering were performed, one in vacuum furnace and another in dilatometer. 15h milled HEA powder has been selected for sintering to study the microstructure and in dilatometer also. Figures 4.10 (a) and (b) show SEM micrographs of sintered sample in vacuum at 1100°C for 1 hr and figures (c) and (d) show indentation after micro hardness test. As sample was pre-compacted and because of pressureless sintering pores were clearly visible in SEM image. Elemental analysis of sintered sample has been done using EDAX. Figure 4.11 shows the elemental mapping of HEA sample and atomic percentage of all the elements have been shown in Table 4.1.

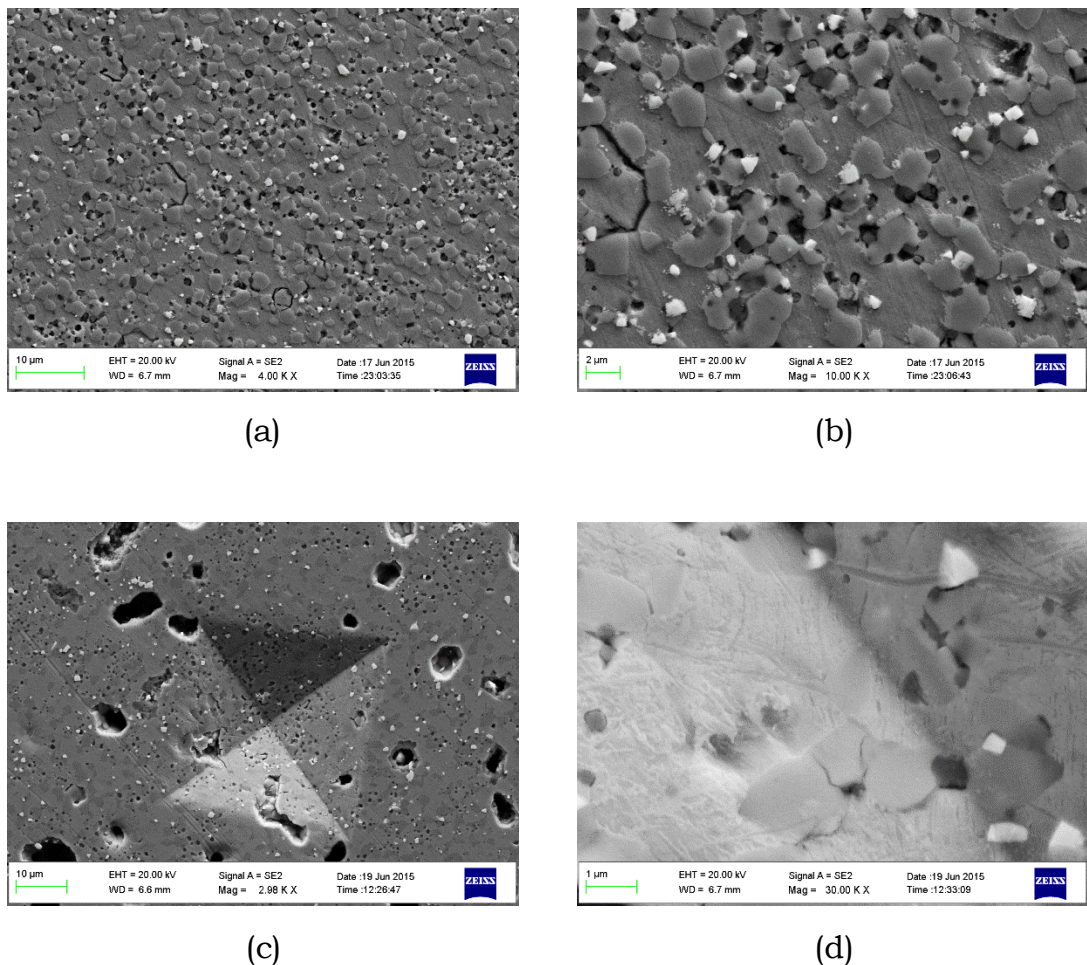


Figure 4-10: SEM micrographs of sintered HEA powder at lower (a) and higher magnification (b); Images of the indentation test at lower (c), and higher magnification (d).

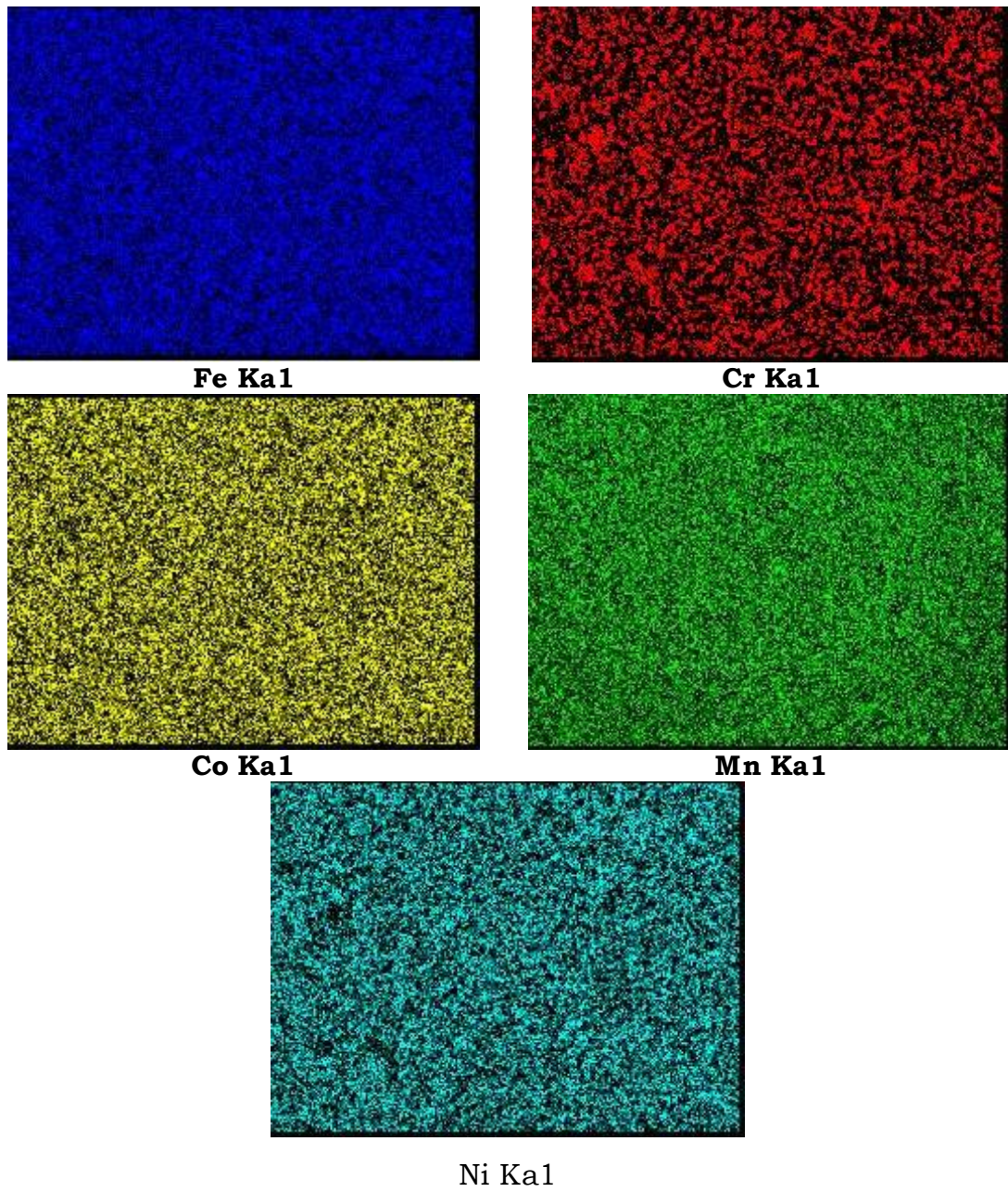


Figure 4-11: Elemental mapping of selected area of sintered HEA sample .

Table 4-1: Quantitative analysis of elements

Elements	Atomic percent
Fe	21.50
Cr	24.37
Co	22.14
Mn	10.12
Ni	21.86

Table 4.2 shows all the dimensions before and after sintering in vacuum furnace. Relative density of sintered sample was around 81% (the theoretical density of as cast HEA that was estimated to be 8.80 g/cm³). Average hardness value of vacuum sintered sample was 305 HV.

Table 4-2: Dimensional measurements of the sintered sample at 1100 °C

15hr HEA	Diameter (mm)	Thicknes s (mm)	Weight (g)	Volume (mm ³)	Density (g/cm ³)
Green	10.17	5.24	2.074	425.44	4.874
Sintered	8.74	3.14	1.3468	188.28	7.153(81%)

Figures 4.12, 4.13, and 4.14 show dilatometer plots of 15 h milled HEA powder sample at different temperatures. When heating was started sample exhibit thermal expansion behavior up to 480°C. However sample did not show perfect linear expansion. Initially it shows very slow expansion up to 262°C with relatively lower expansion. Expansion rate slightly increased up to 480°C and here it shows almost linear behavior. Expansion in the sample stopped at about 480°C and sample started shrinking. Sample shows gradual increase in shrinkage up to about 1000°C. Beyond this temperature, there was a rapid increase in shrinkage. Shrinkage continued till

temperature reached to set value and for an isothermal period of about 30 min. Shrinkage almost stopped after 40 min of holding time.

For study of sintering kinetics data of heating zone, i.e. non-isothermal sintering region was collected. Method to measure the shrinkage has been shown in Fig 4.12 and measured linear shrinkage values have been shown in Fig. 4.15.

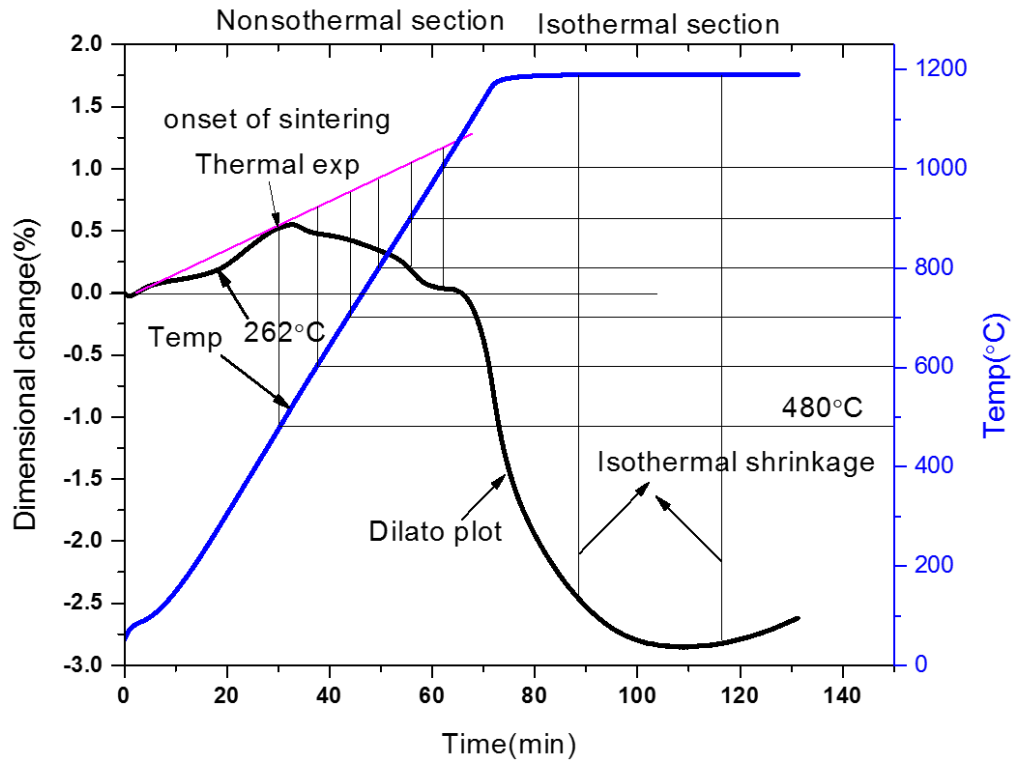


Figure 4-12: Dilatometer plot of the FeCrCoMnNi HEA sample sintered at 1150°C for isothermal holding of 1 h.

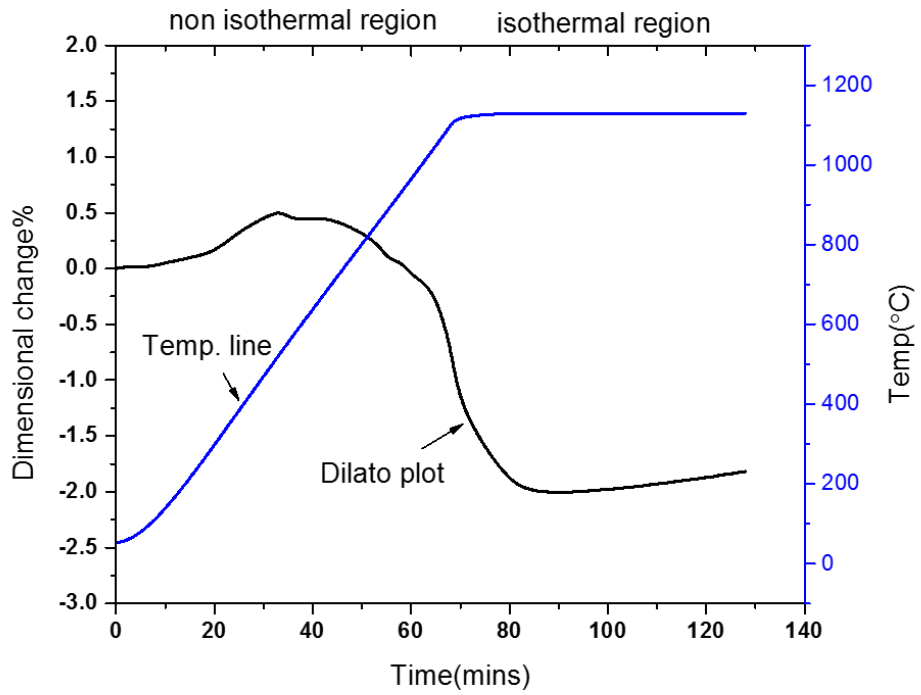


Figure 4-13: Dilatometer plot of the FeCrCoMnNi HEA sample sintered at 1100°C for isothermal holding of 1 h.

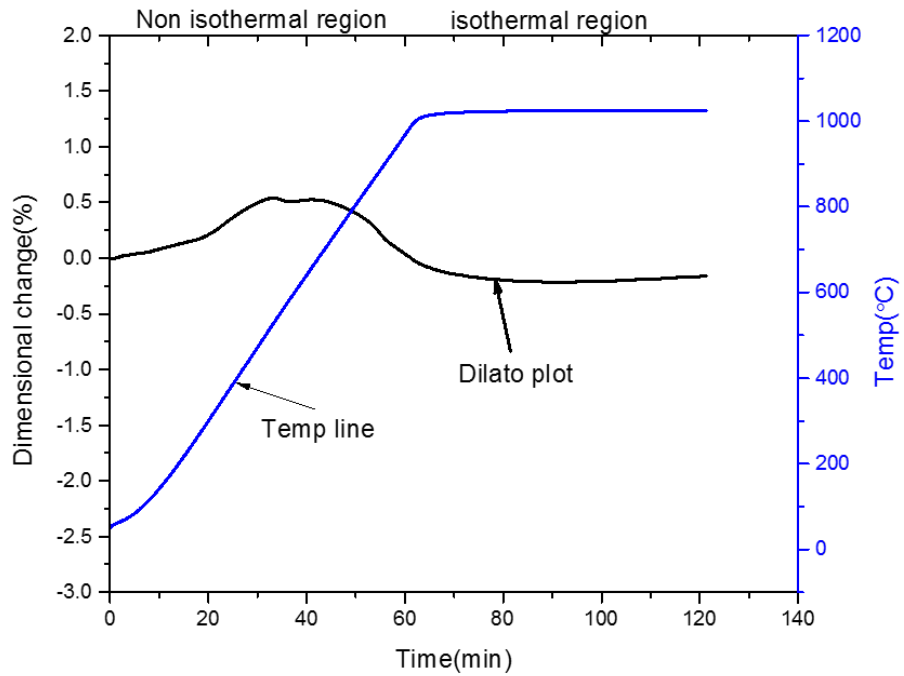


Figure 4-14: Dilatometer plot of the FeCrCoMnNi HEA sample sintered at 1000°C for isothermal holding of 1 h.

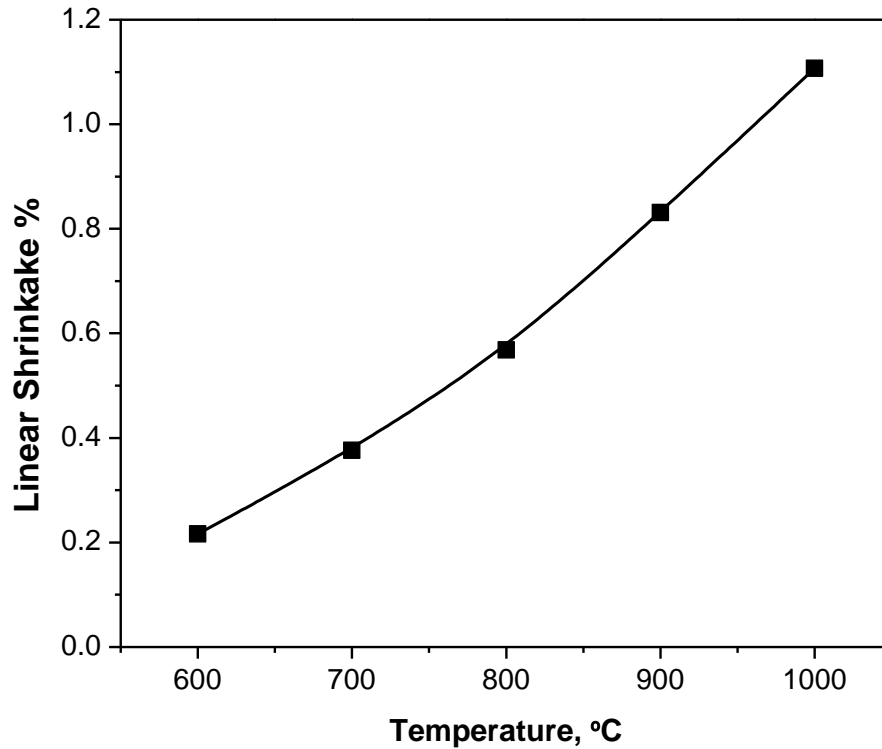


Figure 4-15: Non-isothermal shrinkage obtained from dilatometer curves
 To measure the activation energy of sintering during non-isothermal heating, equation (4.1) was used. Equation (4) is based on the Young and Cutler's equation for densification during a constant heating rate and modified slightly by Han et al. [23].

$$\ln\left(T^p \frac{dY}{dT}\right) = -\frac{Q}{(n+1)RT} + \ln C \quad (4.1)$$

where Y is $\Delta L/L_0$, L_0 is the initial length of the green compact, ΔL is the change in length, T is the temperature, R is the universal gas constant, C is a constant depending on material parameters, n and P are constants. P has the value of 1 for viscous flow (VF), 3/2 for volume diffusion (VD) and 5/3 for grain boundary diffusion (GBD). The values of n are 0, 1 and 2 for VF, VD and GBD respectively. Figures 4.16 to 4.18 show the Arrhenius plot based on equation (4.1) to obtain activation energies.

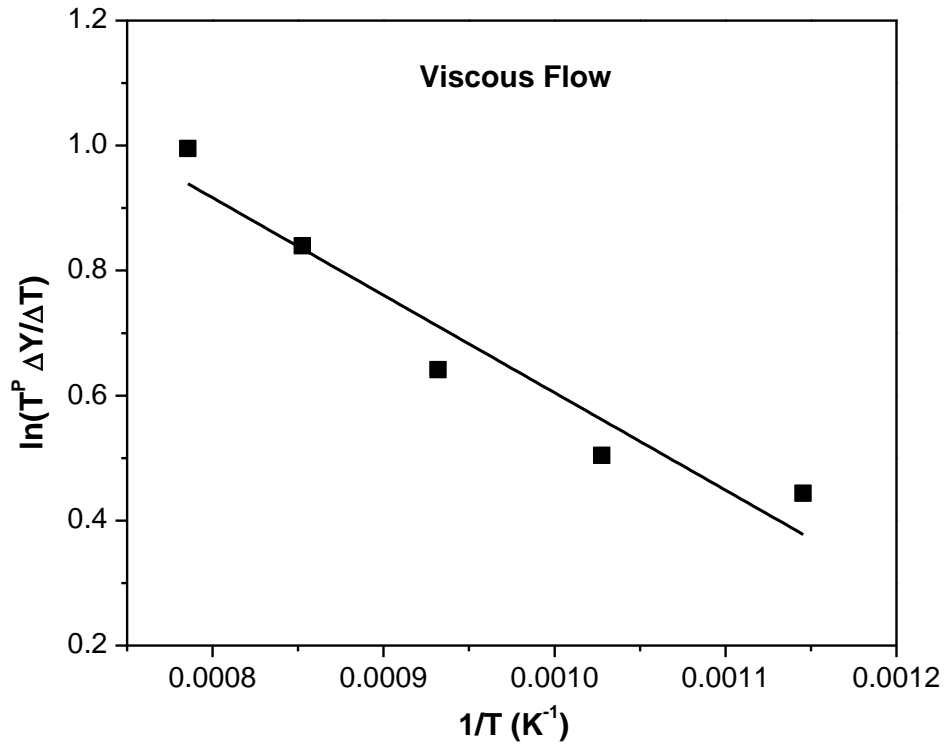


Figure 4-16: Arrhenius plot to estimate activation energy for viscous flow

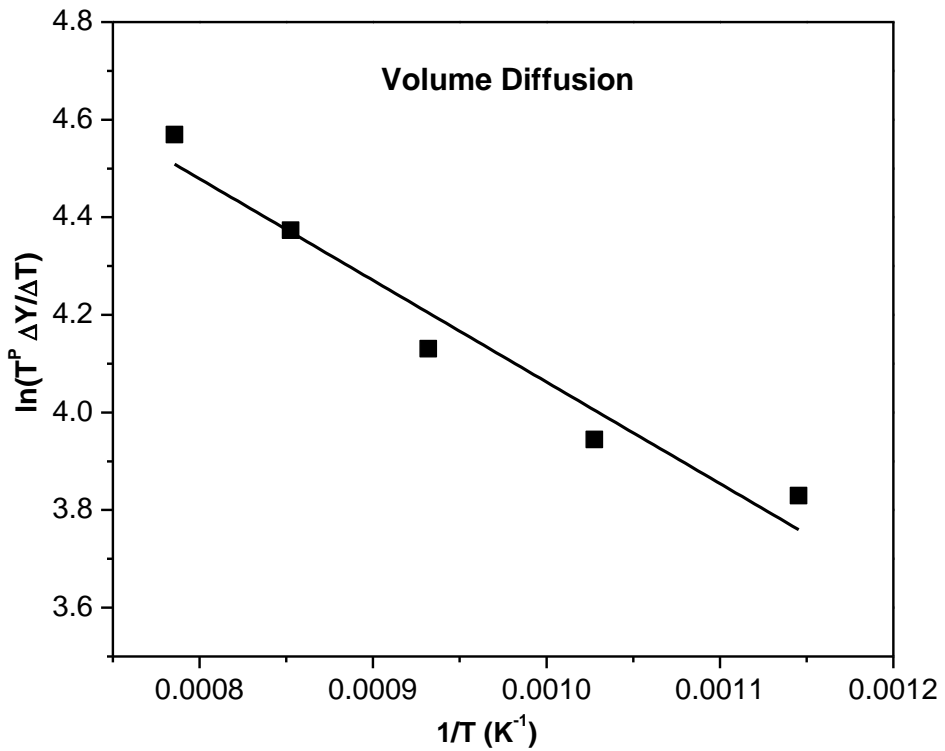


Figure 4-17: Arrhenius plot to estimate activation energy for volume diffusion

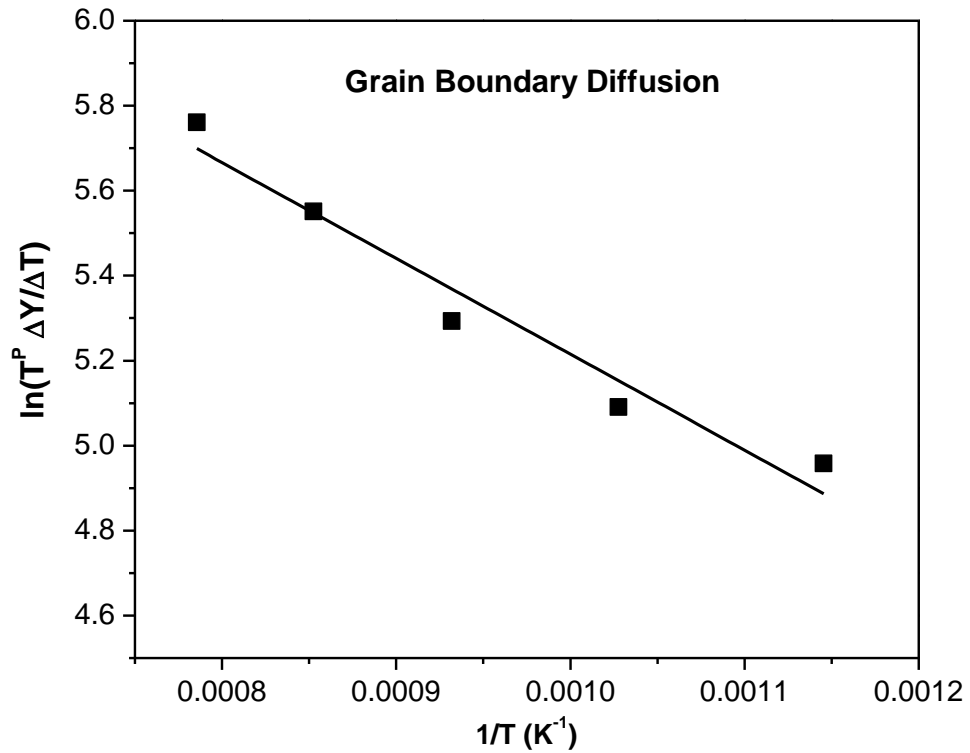


Figure 4-18: Arrhenius plot to estimate activation energy for GBD.

All the values of activation energies for different mechanisms have been given in Table 4.3. These low activation energies indicates that during initial stage of sintering, a large amount of contribution was due to the movement and inhalation of dislocations and defects.

Table 4-3: Activation energies obtained during non-isothermal sintering in the present work

Mechanism	Viscous Flow	Volume Diffusion	Grain Boundary Diffusion
Activation Energy (kJ/mol)	13	37	56

CHAPTER 5

CONCLUSIONS

FeCrCoMnNi HEA alloy has been successfully synthesis by 10h of ball milling. 10h and 15h milled HEA powder shows same behavior indicates phase stability. Heat treatment of alloy suggests stability in phase up to 1100°C. DSC profile indicates the release of internal strains up to about 480°C. The dilatometric studies reveals that the onset of sintering at about 480°C. The activation energies of various possible sintering mechanisms, such as viscous flow, volume diffusion and grain boundary diffusion were estimated during non-isothermal sintering and were found to be 13 kJ/mol, 37 kJ/mol and 56 kJ/mol respectively. These low activation energies indicates that during initial stage of sintering, a large amount of contribution was due to the movement and inhalation of dislocations and defects.

REFERENCES

- [1] B. Cantor, I. Chang, P. Knight, A. Vincent, Microstructural development in equiatomic multicomponent alloys / *Materials Science and Engineering A* 375–377 (2004) 213–218.
- [2] Y. Zhang, T. Zuo, Z. Tang, M. Gao, K. Dahmen, P. Liaw, Z. Lu, Microstructures and properties of high-entropy alloys / *Progress in Materials Science* 61 (2014) 1–93.
- [3] F. Otto, N. Hanold , E. George, Microstructural evolution after thermomechanical processing in an equiatomic, single-phase CoCrFeMnNi high-entropy alloy with special focus on twin boundaries / *Intermetallics* 54 (2014) 39-48.
- [4] Y. Ye, Q. Wang, J. Lu, C. Liu and Y. Yang, Design of high entropy alloys: A single-parameter thermodynamic rule./ *Scripta Materialia* xxx (2015) xxx–xxx.
- [5] M. Brocq, A. Akhatova, L. Perrière, S. Chebini, X. Sauvage, E. Leroy and Y. Champion, Insights into the phase diagram of the CrMnFeCoNi high entropy alloy, *Acta Materialia* 88 (2015) 355–365
- [6] F. Yuhu, Z. Yunpeng, G. Hongyan, S. Huimin, H. Li, AlNiCrFe_xMo_{0.2}CoCu High Entropy Alloys Prepared by Powder Metallurgy *Rare Metal Materials and Engineering*, 2013, 42(6): 1127-1129.
- [7] W. Ji, W. Wang, H. Wang, J. Zhang, Y. Wang, F. Zhang, Z. Fu, Alloying behavior and novel properties of CoCrFeNiMn high-entropy alloy fabricated by mechanical alloying and spark plasma sintering / *Intermetallics* 56 (2015) 24-27.
- [8] S. Varalakshmi, M. Kamaraj, B. Murty, Processing and properties of nanocrystalline CuNiCoZnAlTi ,high entropy alloys by mechanical alloying/ *Materials Science and Engineering A* 527 (2010) 1027–1030.

-
- [9] W. Chen , Z. Fu , S. Fang , Y. Wang , H. Xiao, D. Zhu, Processing, microstructure and properties of $\text{Al}_{0.6}\text{CoNiFeTi}_{0.4}$ high entropy alloy with nanoscale twins /*Materials Science & Engineering A* 565 (2013) 439–444.
- [10] B. Murty, J. Yeh, S. Ranganathan, Chapter 1 - a brief history of alloys and the birth of high-entropy alloys, in: B. M. Y. Ranganathan (Ed.), *High Entropy Alloys*, Butterworth-Heinemann, Boston, 2014, pp. 1 – 12.
- [11] C. Tong, M. Chen, J. Yeh, S. Lin, S. Chen, T. Shun, S. Chang, Mechanical performance of the $\text{Al}_x\text{CoCrCuFeNi}$ high-entropy alloy system with multiprincipal element/, *Metallurgical and Materials Transactions A* 36 (5) (2005) 1263–1271.
- [12] S. Guo, C. Ng, J. Lu, C. Liu, Effect of valence electron concentration on stability of fcc or bcc phase in high entropy alloys/ *Journal of Applied Physics* 109 (10).
- [13] C. Hsua, C. Juana, W. Wang, T. Sheuc, J. Yeh, S. Chend, On the superior hot hardness and softening resistance of $\text{AlCoCr}_x\text{FeMo}_{0.5}\text{Ni}$ high-entropy alloys /*Materials Science and Engineering A* 528 (2011) 3581–3588.
- [14] Y. Zhou, Y. Zhang, Y. Wang, G. Chen, Solid solution alloys of AlCoCrFeNiTi_x with excellent room-temperature mechanical properties/ *Applied Physics Letters* 90 (18) (2007)
- [15] F. Wang, Y. Zhang, Effect of Co addition on crystal structure and mechanical properties of $\text{Ti}_{0.5}\text{CrFeNiAlCo}$ high entropy alloy/ *Materials Science and Engineering: A* 496 (1–2) (2008) 214 – 216.
- [16] Y. Zhou, Y. Zhang, T. Kim, G. Chen, Microstructure characterizations and strengthening mechanism of multiprincipal component $\text{AlCoCrFeNiTi}_{0.5}$ solid solution alloy with excellent mechanical properties/ *Materials Letters* 62 (17–18) (2008) 2673 – 2676.
- [17] J. Jiang, X. Luo, High temperature oxidation behaviour of AlCuTiFeNiCr high-entropy alloy/ *Advanced Materials Research* 652 (2013) 1115–1118.

-
- [18] K. Zhang, Z. Fu, J. Zhang, J. Shi , W. Wang, H. Wang, Y. Wang, Q. Zhang, Annealing on the structure and properties evolution of the CoCrFeNiCuAl high-entropy alloy / *Journal of Alloys and Compounds* 502 (2010) 295–299.
- [19] S. Singh, N. Wanderka, B. Murty, U. Glatzel, J. Banhart, Decomposition in multi-component AlCoCrCuFeNi high-entropy alloy, *Acta Materialia* 59 (1) (2011) 182 – 190.
- [20] N. Tariq, M. Naeem, B. Hasan, J. Akhter, M. Siddique , Effect of W and Zr on structural, thermal and magnetic properties of AlCoCrCuFeNi high entropy alloy / *Journal of Alloys and Compounds* 556 (2013) 79–85.
- [21] H. Chou, Y. Chang, S. Chen, J. Yeh, Microstructure, thermophysical and electrical properties in Al_xCoCrFeNi (0 ≤ x ≤ 2) high-entropy alloys/ *Materials Science and Engineering: B* 163 (3) (2009) 184 – 189.
- [22] P. Bhattacharjee, G. Sathiaraj , M. Zaid, J. Gatti , C. Lee, T. sai, J. Yeh, Microstructure and texture evolution during annealing of equiatomic CoCrFeMnNi high-entropy alloy / *Journal of Alloys and Compounds* 587 (2014) 544–552.
- [23] J.Han, A.M.R.Senos, P.Q.Mantas, Nonisothermal Sintering of Mn doped ZnO / *J. Eur. Ceram. Soc* 19 (1999) 1003-1006.